REFERENCES

1 Malhotra, V.M., Ramachandran, V.S., Feldman, R.F. and Aitcin, P.C., " Condensed Silica Fume in Concrete," CRC Press, Florida, 1987.

2 Powers, T.C. and Helmuth, R., " Theory of volume changes in hardened portland-cement paste during freezing," Highway Research Board, 32nd Annual Meeting, Jan, pp.285-296, 1953.

3 Litvan, G.G., " Frost action in Cement in the presence of de-icers," Cement and Concrete Research, vol.6, no.3, May, pp. 351-356, 1976.

4 Meier, U. and Harnik, A.B., " The freezing of water in Hardened Cement paste in case of prevented evaporation," Cement and Concrete Research, vol.8, no.5, pp.545-551, 1978.

5 Lai, P.S.H., " Study on the Durability of Concrete containing lignite Fly ash," Ph.D thesis, Dept. of Civil Engineering, University of Saskatchewan, Canada, 1989.

6 Sarkar, S.L., Baalbakai, M. and Aitcin, P.C., " Microstructural development in a high-strength concrete containing a Ternary cementitious system," Cement, Concrete and Aggregates, CCAGDP, vol.13, no.2, pp.81-87, winter 1991.

7 Nasser, K.W. and Lai, P.S.H., " Effects of Sulphates on concrete containing fly ash," 2nd CANMET/ACI International Conference on Durability of Concrete, Supplementary papers, pp.817-838, 1991.

8 Mather, B., " How to make concrete that will be immune to the effects of freezing and thawing," Paul Klieger Symposium on Performance of Concrete, ACI SP-122, pp 1-18, 1990.

9 Yuan R.L. and Cook, J.E., " Study of a Class C fly ash concrete," Fly ash, Silica fume, Slag & Other Mineral By-products in Concrete, ACI, SP-79, pp. 307-320, 1983.

10 Neville, A.M., " Properties of Concrete," Pitman publishing, 3rd edition, 1981.

11 Diamond, S., " The Microstructures of Cement paste in Concrete," Proceedings of the VIIIth Intl. Congress on Chemistry of Cement, Rio de Janeiro, pp. 122-147, 1986.

12 Mills, R.H., " Characterization of Fly ash hydration reactions from Microstructure," Proceedings of the Annual Meeting of the Materials Research Society, vol.65, Materials Research Society, Pittsburg, pp. 207-217, 1986.

Table 1. Chemical Analysis and Physical Properties of CSA Type 10 (ASTM Type 1) cement, Saskatchewan Fly ash and Condensed Silica Fume :

Chemical Analysis	Cement		Fly Ash		Silica Fume	
		ASTM C 150		ASTM C 618		CSA.A 23.5
SiO_2	21.19	--	47.40	--	95.41	85.0 min
Al_2O_3	4.10	--	21.5	--	1.09	-
Fe_2O_3	2.34	--	5.3	--	-	-
CaO, total	62.84	--	14.40	--	0.32	
CaO, free	0.99	--				
$SiO_2+Al_2O_3+Fe_2O_3$			74.2	50.5 min	0.24	1.0 max
SO_3	2.56	3.0 max	0.58	5.0 max		
MgO	4.56	6.0 max	2.90	5.0 max	0.73	
Alkalies as Na_2O	0.66		1.77	1.5 max	-	
C_3S	56.6	--				
C_2S	18.1	--				
C_3A	6.90	--				
C_4AF	7.10	--				
Loss on ignition	1.40	3.0 max	0.65	6.0 max	1.80	6.0 max
Moisture content			0.09	3.0 max		
Insoluble residue	0.20	0.75 max				
PHYSICAL PROPERTIES						
Autoclave expansion	0.74	0.8 max	0.13	0.8 max		0.2 max
Time Vicat, minutes	75	45 - 375				
Compressive Strength						
at 3 days, MPa (psi)	24.5(3550)	12.4(1800)				
7 days, MPa (psi)	31.7(4600)	19.3(2800)				
28 days, MPa (psi)	37.0(5370)	27.6(4000)				
45-mm sieve retained, %	0.5	--	26.32	34 max		10 max
Blaine fineness, m^2/Kg	401	--			20,000	
Drying shrinkage increase						
at 28-days, %			0.09	0.03 max		0.03 max
Specific gravity			2.21	--		
Pozzolanic Activity Index:						
with portland cement at					119.1	85 min
28 days, % of control			82.00	75.0 min		
with lime at 7 days (psi)			871	800 mix		
Water Requirement:						
% of control			94	105 max	139	

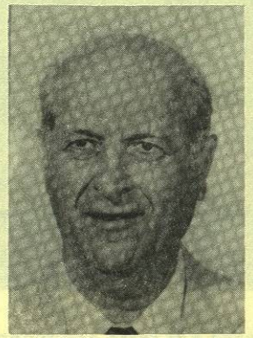

Karim W. Nasser,
Professor, Dep. of Civil Engineering, University of Saskatchewan, Saskatoon, Canada

Table 2. Proportions of Concrete Mixtures and Properties of Fresh and Hardened Concrete

Mix No.	Fly ash wt. %	Cementitious Materials Kg/m³			w/c	super-plasti-cizer Kg/m³	Air %	K-slump mm	Unit weight Kg/m³	Compressive Strengths (MPa) (ave. of 5-75 x 150 mm cylinders)		
		cement	flyash	CSF						5 hrs*	28days	56days
HP-C0	-	393.2	0.0	0.0	0.28	11.8	-	35	2494.3	32.1	44.3	54.4
HP-C1	-	365.1	0.0	40.5	0.28	12.0	-	38	2526.8	59.0	66.7	68.0
HF-20	20	278.3	79.6	39.8	0.27	7.78	-	35	2503.1	56.7	72.1	69.3
HF-35	35	210.0	134.4	38.6	0.27	7.55	-	35	2429.6	37.7	56.1	59.3
HF-50	50	156.4	193.4	39.3	0.27	7.67	-	38	2468.5	28.9	53.4	55.4
HF-60	60	117.0	233.9	39.4	0.27	7.69	-	25	2475.6	15.9	54.1	54.8
HF-70	70	76.9	273.5	39.3	0.26	6.51	-	35	2472.0	12.0	41.7	42.1
HF-80	80	39.4	312.6	38.9	0.25	6.95	-	20	2443.8	4.4	27.9	34.2
HA-20	20	273.2	78.1	39.0	0.27	9.96	4.3	35	2450.9	-	67.5	70.6
		264.2	75.5	37.7	0.27	9.63	8.2	40	2369.6	-	57.4	66.6
HA-50	50	154.7	193.2	38.7	0.27	9.87	4.4	20	2429.7	-	50.5	58.3
		145.0	181.1	36.3	0.27	9.25	8.7	40	2277.8	-	48.3	49.7

* For 5-hour accelerated curing, the strength was calculated as the average of 3-75x150 mm cylinders.
Aggregate to cement ratio was maintained at 5.0.
Coarse aggregate to fine aggregate ratio was maintained at 1.22.
Maximum size of coarse aggregates was 3/4 in. (20 mm).

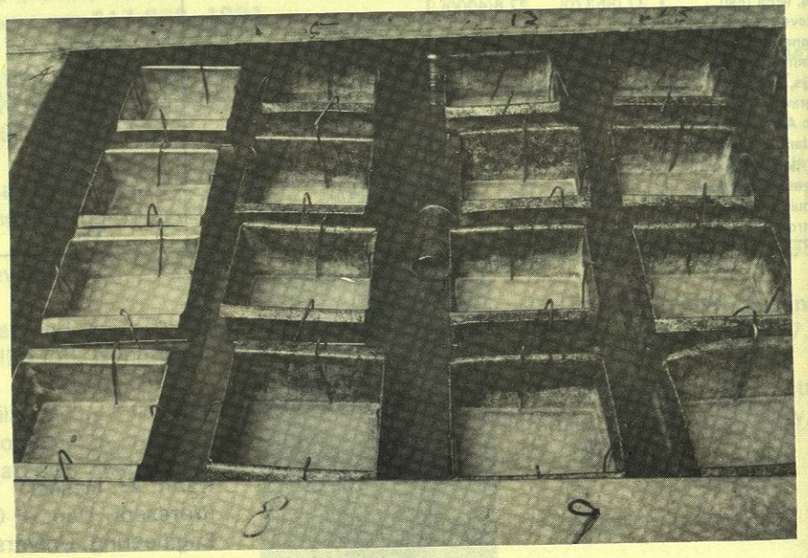

Fig. 1. Specimens in metal containers in the Freezing and thawing Tank.

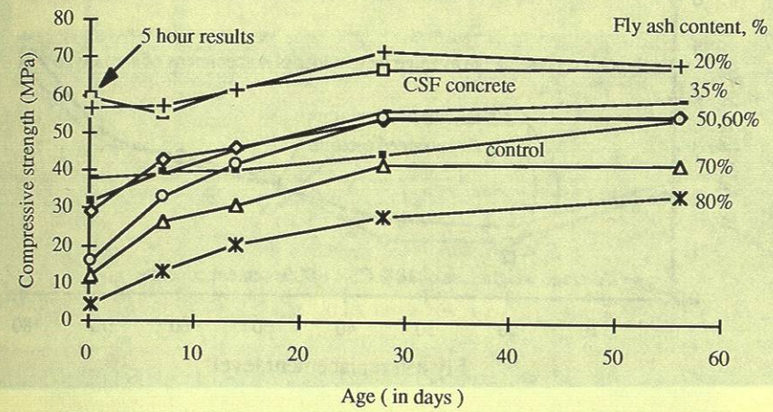

Fig. 2. Compressive strength of concrete versus Age.

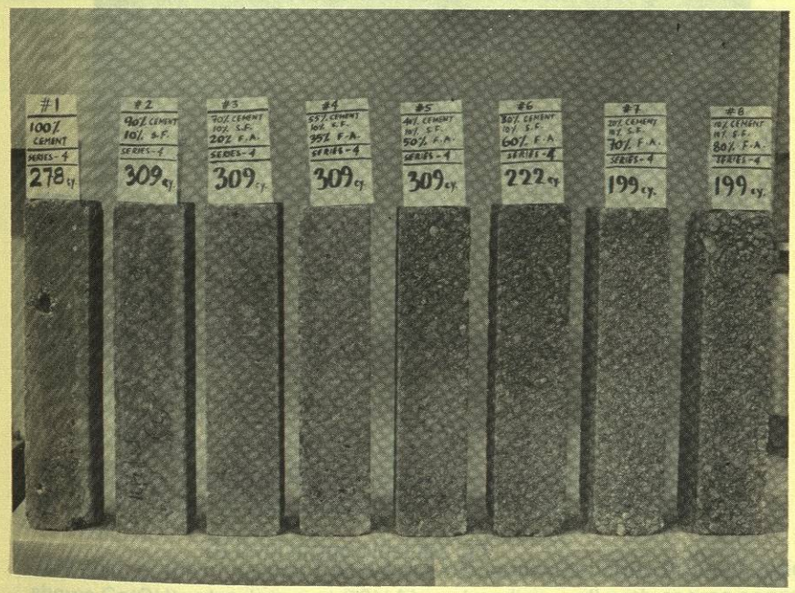

Fig. 3. Non air-entrained Concrete specimens after the Freezing and thawing test.

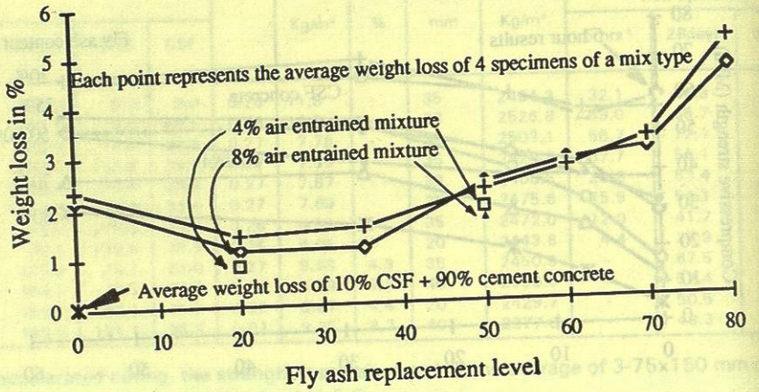

Fig. 4. Average weight loss of freezing and thawing specimens versus mixture ty

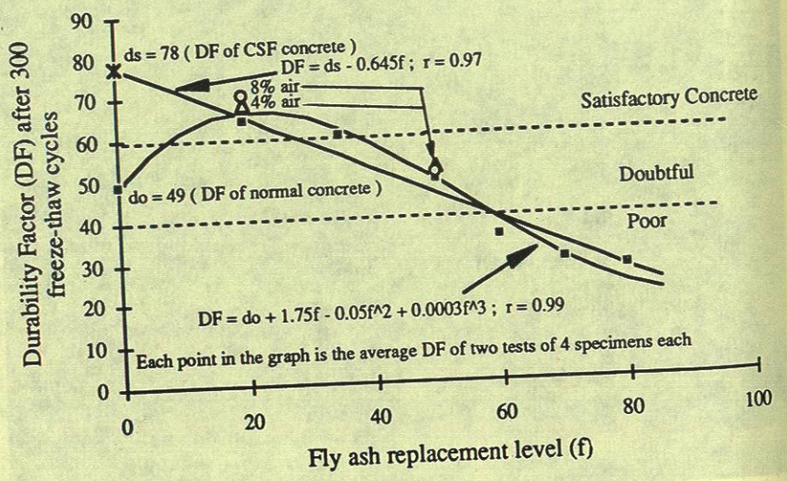

Fig. 5. Durability Factor (DF_{300}) vs. Fly ash replacement levels.

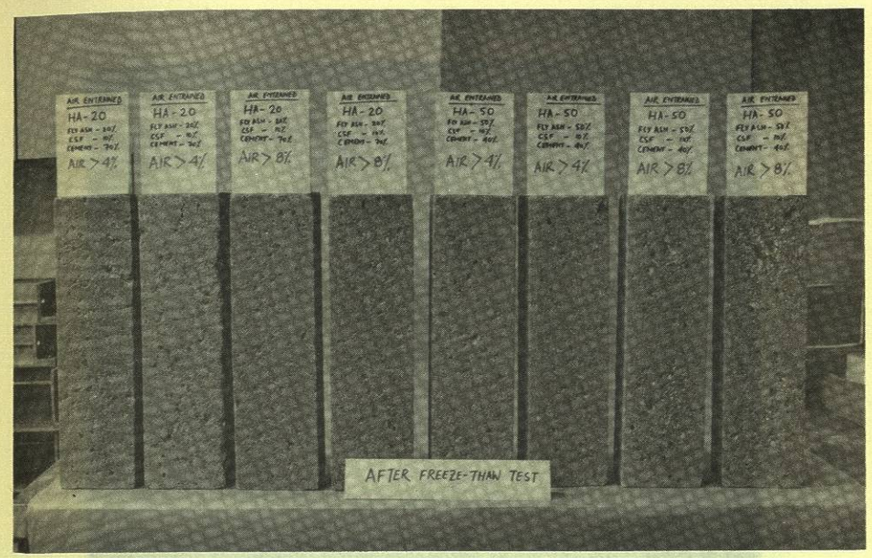

Fig. 6. Air-entrained Concrete specimens after the Freezing and thawing test.

Fig. 7. SEM micrograph of normal 100% type 10 cement-concrete [Magnification x 1850], shows $Ca(OH)_2$ platelets and CSH fibres bonding well with coarse aggregates after 28-days of curing.

Fig. 8 SEM micrograph of 20%flyash + 10%CSF concrete after 28days moist curing Magnification x 1850.

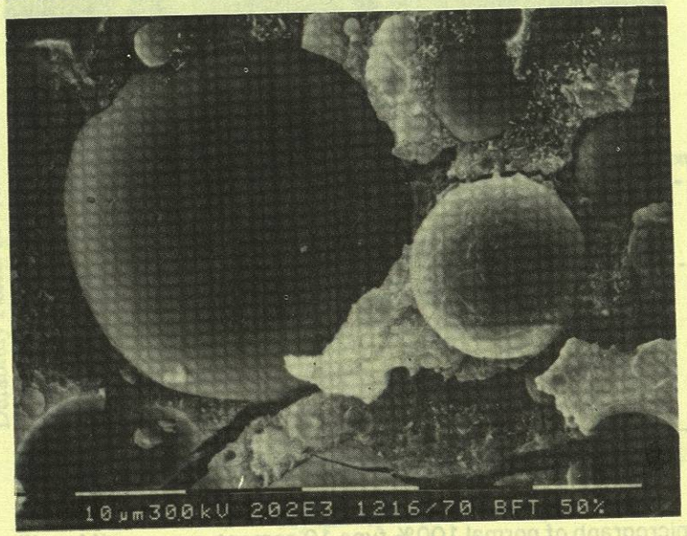

Fig. 9. SEM micrograph of high flyash concrete (50%flyash + 10%CSF), reveals bond of unreacted flyash with the paste separated by a fine gap [Magnification x 202

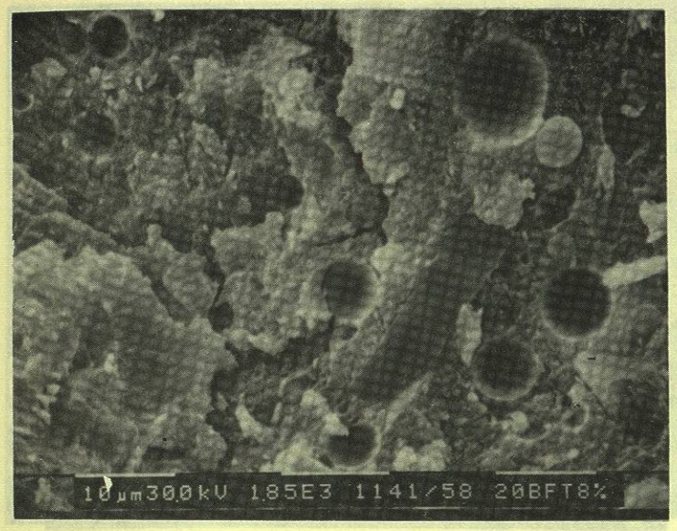

Fig. 10. SEM micrograph of 20%flyash + 10%CSF concrete after 28days moist curing containing 8.2% entrained air; Magnification x 1850.

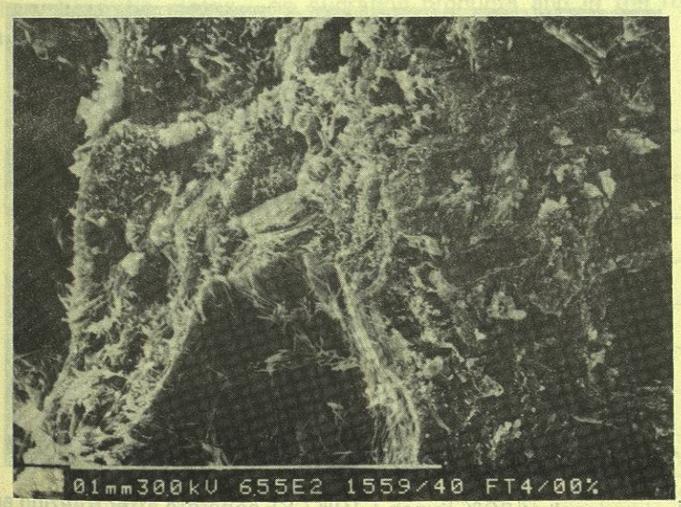

Fig. 11. SEM micrograph of normal concrete after freezing and thawing test [Magnification x 655]. Heavy deposition of whitish $Ca(OH)_2$ and radial growth of hydration products evident.

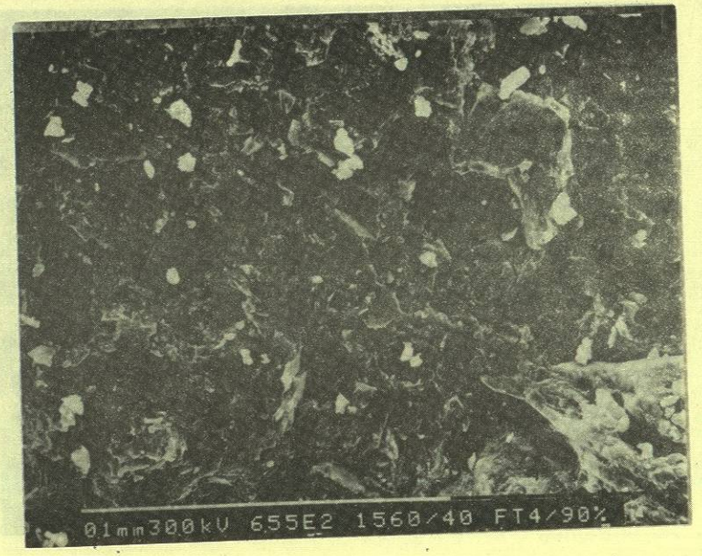

Fig. 12. SEM micrograph of silica fume concrete after freezing and thawing [Magnification x 655]. Dark, dense matrix with absence of radial growths.

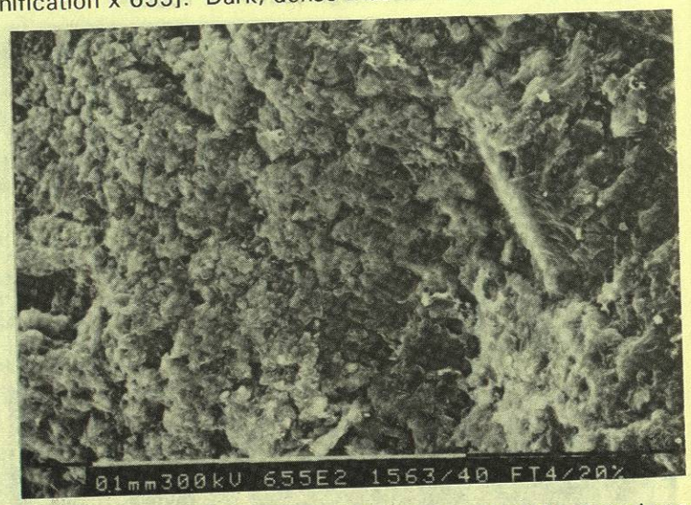

Fig. 13. SEM micrograph of 20% flyash + 10%CSF concrete after freezing and thawing [Magnification x 655]. Fairly dense CSH matrix, formed by consumption of $Ca(OH)_2$ in secondary pozzolanic reactions. Platy $Ca(OH)_2$ and rounded unreacted flyash particles, absent.

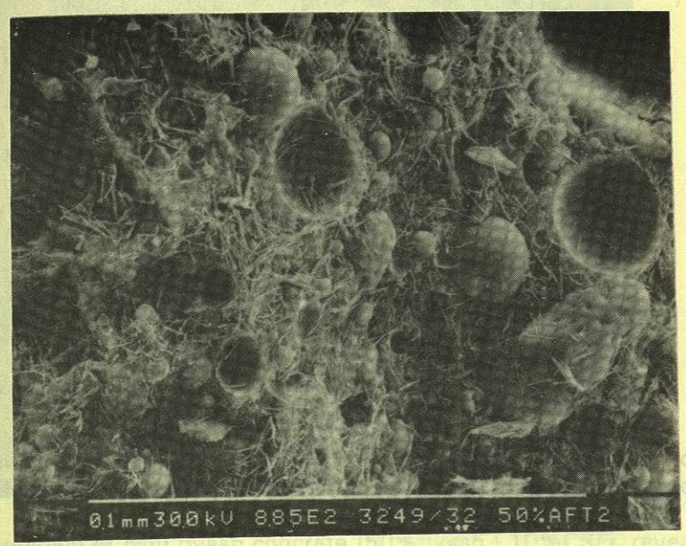

Fig. 14a SEM micrograph of high flyash (50%) + 10%CSF concrete after freezing and thawing test [Magnification x 885]. Needle-like crystals of ettringite scattered throughout the matrix - on hydration products and in the rounded sockets of unreacted flyash particles.

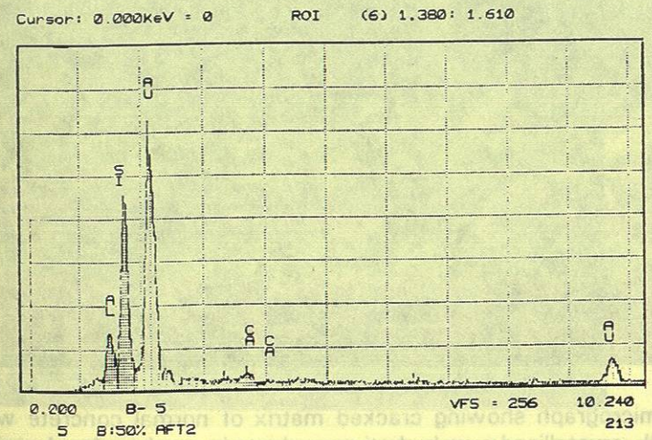

Fig. 14b EDS of the surface of a rounded unreacted fly ash particle of Fig. 14a (Al-aluminium, Ca-calcium, Si-silicon, Au-gold coating)

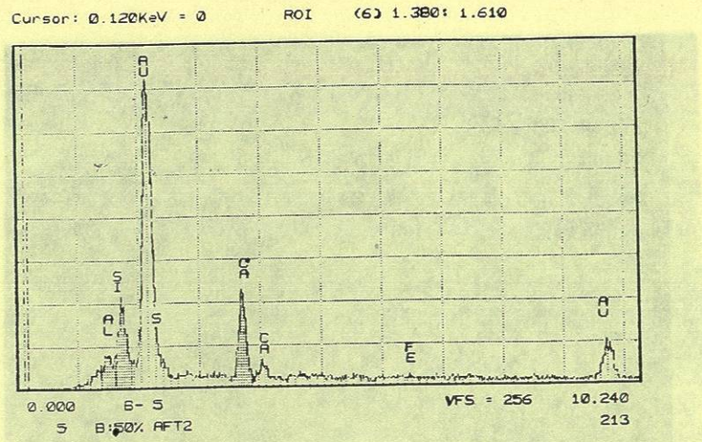

Fig. 14c EDS of the needle-like ettringite in matrix of Fig. 14a (Al-aluminium, Ca-calcium, S-sulphur, Si-silicon, Au-gold coating)

Fig. 15. SEM micrograph showing cracked matrix of normal concrete with platelets of $Ca(OH)_2$ crystallised over hydration products in cracks, after freezing and thawing cycles [Magnification x 1310]. Some needle-like ettringite crystals are also observed.

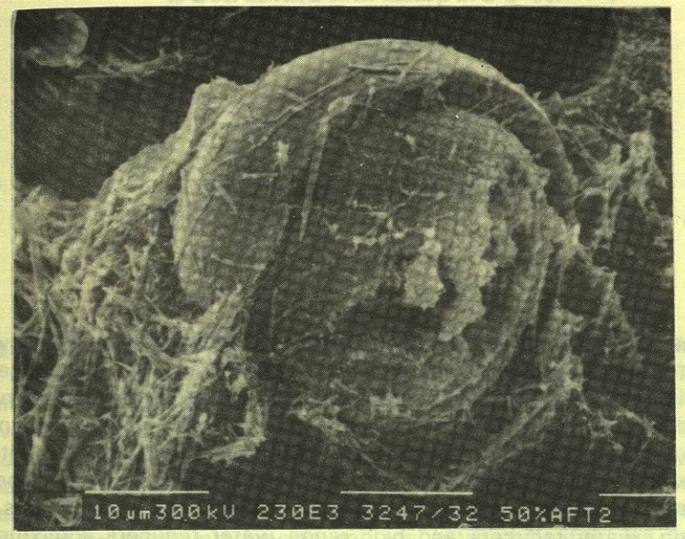

Fig. 16. SEM micrograph of high flyash concrete (50%flyash + 10%CSF), reveals a partly reacted flyash particle with its envelope broken and with needle-like crystals of ettringite scattered around, after 300 freezing and thawing cycles [Magnification x 2300].

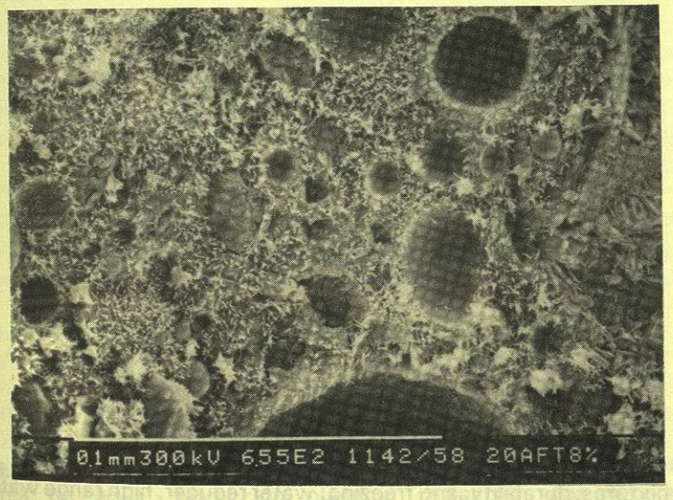

Fig. 17. SEM micrograph of 20% flyash + 10% CSF air-entrained concrete reveals a matrix with numerous air-void sockets filled with needle-like crystals, after 300 freezing and thawing cycles [Magnification x 655].